Mitochondria Morphology and DNA Content upon Sublethal Exposure to Beta-Amyloid$_{1–42}$ Peptide

Andrea Diana[1], Goran Šimić[2], Elena Sinforiani[3], Nicola Orrů[1], Giuseppina Pichiri[4] and Giorgio Bono[5]

[1]Department of Cytomorphology, University of Cagliari, Cittŕ Universitaria di Monserrato, Monserrato, Italy
[2]Department of Neuroscience, Croatian Institute for Brain Research, School of Medicine University of Zagreb, Zagreb, Croatia
[3]Istituto di Ricovero e Cura a Carattere Scientifico (IRCCS) Neurologico C. Mondino, Pavia, Italy
[4]Department of Sciences Applied to Biosystems, University of Cagliari, Cittŕ Universitaria di Monserrato, Monserrato, Italy
[5]Department of Neuroscience, University of Insubria, Varese/IRCCS C. Mondino, Pavia, Italy

ABSTRACT

Brains affected by Alzheimer's disease (AD) show a large spectrum of mitochondrial alterations at both morphological and genetic level. The causal link between amyloid beta peptides (Ab) and mitochondrial dysfunction has been established in cellular models of AD using Ab concentrations capable of triggering massive neuronal death. However, mitochondrial changes related to sublethal exposure to Ab are less known. Here we show that subtoxic, 1 mMAb1–42 exposure does not change the mitochondrial shape of living cells, as visualized upon the uptake of the non-potentiometric fluorescent probe Mitotracker Green and enhanced yellow fluorescent protein (EYFP)-tagged cytochrome c oxidase expression. Immunolocalization of oxidative adducts 8-hydroxy-2'-deoxyguanosine, 8-hydroxyguanine and 8-hydroxyguanosine demonstrates that one-micromolar concentration of Ab1–42 is also not sufficient to elicit dramatic qualitative changes in the RNA/DNA oxidative products. However, in comparison with controls, semi-quantitative analysis of the overall mitochondrial mass by integrated fluorescence intensity reveals an ongoing down-regulation in mitochondrial biosynthesis or, conversely, an enhanced autophagic demise of Ab treated cells. Furthermore, a significant increase of the full-length mitochondrial DNA (mtDNA) from Ab-treated versus control cells is found, as measured by long range polymerase chain reaction (PCR). Such up-regulation is accompanied by extensive fragmentation of the unamplified mtDNA, probably due to the detrimental effect of Ab. We interpret these results as a sequence of compensatory responses induced by mtDNA damage, which are devoted to repression of oxidative burst. In conclusion, our findings suggest that early therapeutic interventions aimed at prevention of mitochondrial oxidative damage may delay AD progression and help in treating AD patients.

Key words: amyloid toxicity, mitochondrial DNA, neuroblastoma cell culture, oxidative stress

Introduction

Alzheimer's disease (AD) is a late-onset, progressive, age-dependent neurodegenerative disorder whose biological hallmarks reside in the progressive formation of amyloid plaques and neurofibrillary tangles[1,2], ultimately leading to synaptic failure, disconnection syndrome and neuronal cell death, which are clinically manifested by the impairment of cognitive functions and changes in behavior and personality[3]. Advancements in molecular, cellular and animal models of AD, as well as post-mortem examination of brain neurons from AD patients, have revealed that the formation of beta-amyloid (Ab) peptides and their entrance into mitochondria are the prominent factors in cellular changes in the AD brain because they induce the generation of free radicals and oxidative damage in AD brain[4,5]. Since neuronal viability is highly dependent on oxidative energy metabolism[6], the impaired mitochondrial functions are having an enormous influence on AD manifestation and progression. Beta-amyloid peptides increase the intracellular generation of reactive oxygen species (ROS), particularly hydrogen peroxide (H_2O_2), thus making mitochondria both targets and sources of oxidative stress[7,8]. In turn, oxygen derived molecules give rise to oxidative adducts, such as 8-hydroxy-2'-deoxiguanosine (8OHdG)[9,10], as a part of mitochondrial DNA (mtDNA) isolated from AD brains. Higher levels of OHdG have been found at the initial stages of AD in postmortem brain sections by means of immunocytochemistry and the detection of oxidized nucleic acids was shown to be reduced with disease progression[11,12]. The pioneering paper by Suter and Richter[13] identified that fragmented mtDNA is the predominant carrier of oxidized DNA bases and presence of 8OHdG. Other studies addressing prominent features of vulnerable neurons in AD have revealed a significant reduction of cytoplasmic area covered by intact mitochondria, which is balanced by up-regulating both average size and total mitochondrial DNA (mtDNA) in individual cells[14]. Moreover, as revealed by in situ hybridization and immunocytochemistry in the very same brain section, the overlap in localization of mtDNA D5kb and 8OHdG seemed to support an intimate relationship between neuronal oxidative damage and dysmorphic mitochondria. In contrast, in most AD cases examined by de la Monte and collaborators[15] the mean level of mtDNA was found to be significantly lower than in the control group. These data have been corroborated by the findings that in AD cells mtDNA content was higher in cybrids that harbor low to medium levels of 4977 bp-deleted mtDNA[16]. In addition, oxidative stress induced by sublethal concentrations of hydrogen peroxyde has been found to cause an increase in mtDNA content that correlates with a larger amount of functional mitochondria[17,18]. The quantitative relevance of toxic inducers has been recently confirmed by the ability of micromolar concentrations of hydrogen peroxide to provoke true oxidative lesion of genomic DNA[19]. However, experimental data on mtDNA is still missing. Interestingly, while neurodegeneration can be observed with very low doses of Ab, a dramatic viability drop in non-primary neuronal cultures is induced only by concentrations greater than 10 mM of $Ab_{1–40}$, thus allowing the definition of a threshold for the so-called subtoxic level of Ab[20].

Our current investigation was aimed to: 1) assess whether sublethal doses of $Ab_{1–42}$ could provoke specific alterations to mitochondria both with regard to morphological and quantitative features and DNA content, 2) determine if genetic and structural changes occur concomitantly, and 3) verify if DNA oxidation at mitochondrial or nuclear level can be triggered by low doses of $Ab_{1–42}$.

Materials and Methods

Cell cultures

Neuroblastoma cell lines (clone SH-SY5Y) were grown in Minimal Essential Medium (MEM) containing Earle's salt supplemented with 10% heat inactivated fetal bovine serum (FBS), 2 mM L-glutamine, 1% non-essential amino acids, streptomycin (100 mg/mL)/penicillin (100 U/mL) (all reagents from Invitrogen, Gaithersburg, MD, USA) and maintained at 37°C in a humid atmosphere with 5% CO_2. One week after seeding when cells reached about 80% confluence, they were exposed to $Ab_{1–42}$ peptide acetate or chloride salt (Recombinant Peptide Technologies, Athens, OH, USA) dissolved in ultra-pure water and previously incubated for 4 days at 37°C (in order to ensure formation of fibrils necessary for toxic induction). Finally, cells were treated for 24 hr with 1 mM $Ab_{1–42}$ in complete medium without FBS.

Gene transfection

Enhanced yellow fluorescent protein (EYFP)-tagged cytochrome c oxidase subunit IV gene has been used to target mitochondrial matrix[21,22]. SH-SY5Y cells were stably transfected with Lipofectamine 2000 (Invitrogen) by selection with the antibiotic G418 (Invitrogen) and then exposed to $Ab_{1–42}$ as referred above.

Mitochondria labeling

After 24-hr $Ab_{1–42}$ exposure, neural cells were washed twice with PBS and supravitally stained with 400 nM Mitotracker Green fluorescent marker (Molecular Probes, Eugene, OR, USA) diluted from 1 mM DMSO stock solution. Cells were washed with medium and observed using a Zeiss Axioskop microscope (Zeiss, Oberkocken, Germany) equipped with differential interference contrast optics, planachromatic objective lenses (40x/0.75 Na water immersion) and standard filters adapted for Mitotracker (460–500 BP excitation, 505 splitter, 510–560 BP emission). Grayscale images were acquired by a 8-bit cooled CCD camera (Sensicam, PCO Computer Optics, Kehlheim, Germany) with a 1280x1024 pixel chip. Image analysis was performed using the Image-Pro Plus software (Media Cybernetics, Silver Spring, MD, USA).

Immunocytochemistry

A monoclonal mouse antibody against oxidative adducts 8-hydroxy-2'-deoxyguanosine, 8-hydroxyguanine, and 8-hydroxyguanosine (anti-8OHdG) was used as a marker of DNA (both genomic and mitochondrial) and RNA oxidative damage (Autogen Bioclear, Calne, UK). Neuroblastoma cells were fixed in periodate-lysine-paraformaldehyde (PLP) for 15 min at 37°C. After rinsing with PBS containing 0.2% Triton X-100, 10% normal goat serum (NGS) (Vector Laboratories Inc., Burlingame, CA, USA) was applied for 1 hr at room temperature (RT). Then, anti-OHdG antibody (5 mg/mL) diluted in PBS containing 0.3% Triton X-100 and 2% NGS was added for 24 hr at RT. After an extensive washing with PBS, samples were incubated for 40 min at RT with fluorescein (FITC) conjugated anti-mouse antibody (Jackson Immunoresearch Labs, West Grove, PA, USA), and rinsed with PBS. Nuclear morphology was evaluated by DAPI staining (5 mg/mL; Molecular Probes, Eugene, OR, USA) for 5 min at RT. Cell imaging and analysis were performed as described above.

DNA extraction

Cells were scraped, centrifuged at 500x g for 10 min and resuspended in extraction buffer composed of 10mM Tris-HCl (pH 8), 100 mM EDTA (pH 8), 20 mg/mL RNAse, 0.5% SDS

and 0.1 mg/ml proteinase K. The samples were then gently shaked for 18 hr at RT. DNA extraction was carried out at 4°C according to Blin and Stafford[23], with some modifications. First, an equal volume of phenol/ chloroform/isoamyl alcohol 25/24/1 mixture was added. Upon centrifugation (1500x g, 10 min), the aqueous phase was transferred to a new tube with an equal amount of chlorophorm/isoamyl alcohol 24/1 and then centrifuged again. DNA was precipitated by adding 0.3M sodium acetate, pH 5.2 (1 volume), 100% cold ethanol (2 volume), then air dried and immediately dissolved in ultra-pure water.

Long extension Polymerase Chain Reaction (LX-PCR)

Long extension PCR for amplification of the entire mitochondrial genome was carried out using outwards primers located in the cytochrome b gene[8] that correspond to the following sequences:
5'-TGAGGCCAAATATCATTCTGAGGGGC-3'
(forward primer, 15148-15174 bp) and
5'-TTTCATCATGCGGAGATGTTGGATGG-3'
(reverse primer, 14841-14816 bp), to generate a 16231 bp molecule.
The reaction components (25 mL) consisted of 0.5 mM dNTPs (Pharmacia, Uppsala, Sweden), 0.3 mM primers (MWG-Biotech, Firenze, Italy), 100 ng genomic DNA as a bottom phase. This master mix was overlaid with 25 mL of 1x buffer and 2.5 Us enzyme mixture (Expand long template PCR system, Roche Diagnostics GmbH, Mannheim, Germany). Thermo-cycling profile involved the following steps: 1) initial denaturation (92°C, 2 min), 2) denaturation (92°C, 10 sec), annealing (70°C, 30 sec), extension (68 °C, 12 min), for a total of 10 cycles, 3) denaturation (92°C, 10 sec), annealing (70°C, 30 sec) with increasing annealing time by 20 sec increments in each successive cycle, extension (68°C, 12 min), for a total of 20 cycles, and 4) final extension (68°C, 7 min). PCR products were loaded onto a 0.4% MP agarose gel (Roche Diagnostics GmbH, Mannheim, Germany) in 1x Tris-Acetate-EDTA (TAE) at 25 V for 18 h. Finally, gel was stained with Sybr Green (Molecular Probes, Eugene, OR, USA) according to the manufacturer instructions.

In order to avoid possible quantitative differences due to methodological reasons several DNA purified samples were amplified and run on the same gel in the same electrophoresis chamber.

Determination of mitochondrial mass and statistics

All of the experiments have been repeated at least three times. Mitochondrial mass was evaluated by measuring the integrated fluorescence intensity of mitochondrial profiles stained by Mitotracker dye under assumption that dye is insensitive to differences in potential. Due to the considerable skewness of distributions, data comparisons were made using the non-parametric test of Kruskal-Wallis with a significance level of $p<0.05$.

Results

Although Ab-treated cells were having higher levels of oxidative damage (see below), both control (Figure 1a) and Ab-treated cells (Figure 1b) showed bright immunofluorescence for 8OhdG and appeared relatively similar. As to the cytological distribution of oxidative adducts, again in both Ab-treated and control cells 8OHdG was mainly concentrated in the cytoplasmic domain with peaks of fluorescence in the perinuclear area, whereas nuclei showed a very weak immunolabeling. In addition, the largest cells displayed a granular immunolocalization regardless of Ab exposure, probably as a consequence of the segregation

of oxidative DNA/RNA adducts within organelles (e.g. ribosomes and mitochondria). Fluorescent traces were also present along the emergence of neuronal processes that soon disappeared at longer distance.

Morphological analysis was based on mitochondrial staining by Mitotracker uptake and EYFP cytochrome c oxidase transfected cells. Mitochondria of control cells labeled with Mitotracker were highly fluorescent. Fluorescence was distributed throughout the cytoplasm apparently in conjunction with a reticular organization of filamentous profiles (Figure 2a). However, despite the continuity of mitochondrial network, Mitotracker load was often variable from cell to cell. Due to the inherent properties of Mitotracker used, this phenomenon could not be ascribed to fluctuations of mitochondrial potential. Uneven distribution of the dye was quite similar to the one observed in mitochondria of Ab treated samples (Figure 2b). We therefore measured the integrated area of several fluorescent mitochondria. In comparison to controls (7664, 9275.9, 8036.2), we found a significant decrease in median values of the randomly selected and examined Ab samples (7368.7, 4812.6, 7462.55, respectively). Alterations of mitochondrial network were absent in Ab exposed cells, as confirmed by incubation with an excess of phosphate salts that triggered a robust swelling accompanied by extensive fragmentation of mitochondria (Figure 2c).

By means of transfection, in neuronal cells containing mitochondria tagged with EYFP, the import of the cytochrome oxidase subunit IV into the mitochondrial matrix resulted in a specific mitochondrial morphology. Our data showed a fluorescent pattern overlapping with Mitotracker stained mitochondria (Figure 3a). In addition, mitochondria filaments extended their localization to neuritic processes. The exposure to 1mMAb seemed to be ineffective at inducing mitochondria to become fragmented or swollen (Figure 3b). Observed enlargements could be occasionally distinguished along mitochondrial strings, but were independent to the Ab treatment.

Results of LX-PCR experiments showed the single distinct band corresponding to ~16.3 kb of the entire mitochondrial human genome (Figure 4). Interestingly, the sharp band (16.3 kb) obtained with the two Ab samples was roughly double in thickness compared to the correspondent mtDNA of control cells. In addition, PCR products from Ab treated cells consisted of a smear of fragments with higher and lower average length plus two more fragments with very low molecular weight. Such findings were not replicated with amplified DNA from control cells. Moreover, electrophoresis of mtDNA showed a higher background which was representative of random DNA fragmentation when the neuroblastoma cells had been cultured in presence of the toxic peptides.

Discussion

During last several years the relationship between mitochondria dysfunctions and Ab accumulation have gained increasing interest due to pivotal role of mitochondria in the AD neurodegenerative process[25–27].Within this framework, one of the major issues is an unpredictable time window between Ab driven plaque formation and the occurrence of clinical symptoms of AD. In search of initial signals affectingmitochondrial architecture and mtDNA content, we designed an experimental model where low dose exposure to $Ab_{1–42}$ was well below the threshold for inducing immediate cell death, but still high enough for the induction of subtle cellular changes.

The main finding of this study is that total mtDNA content was up-regulated in Ab treated cells compared to control cells, as revealed by LX-PCR. The extensive increase of mtDNA was also accompanied by a higher degree of fragmentation, as visualized by a more evident smear of DNA and thicker bands of DNA with low molecular weights. These findings indicate that DNA synthesis may occur concomitantly with a diffuse degradation of

mitochondrial genome. This is consistent with previous reports where the increase of mtDNA and mitochondria has been interpreted as one of the molecular events gearing the cells up to cope with mild to medium stress[17,18]. However, when cells are overwhelmed by high oxidative stress, due to the impaired replication of mtDNA and biogenesis of mitochondria, such a physiological switch may be no longer be effective.

A measurement of total mtDNA in a pure population of neuronal cells has not been extensively studied. The only two papers[14,15] that have systematically addressed the variability of mtDNA content in postmortem AD brains ended up with conclusions that are difficult to resolve. The first group reported a reduction of mtDNA in AD that positively correlated with an increase in mtDNA fragmentation, but was »paradoxically« linked to the increase of mitochondrial mass[14]. On the other hand, although total mtDNA in AD was increased in several neuronal populations, much of this mtDNA was present in digestive organelles and therefore potentially unsuitable for extraction and amplification, as observed by the other group[15]. Due to the reduced numbers of intact mitochondria the amount of amplifiable mtDNA was also reduced[15]. We think that those divergent and controversial results might be explained on the basis of different methodological approaches. Namely, at least some of the differences obtained could be attributed to excessive glial cell reaction associated with cell loss or proliferation of mitochondria in degenerating neurons, which could also heighten the overall mitochondrial genetic content. In our study, we were confident that the specificity of the primers within the highly conserved cytochrome b gene made the LX-PCR method qualitatively reliable for the amplification of a linear product equivalent to the entire mitochondrial genome[24], what allows the detection of mutational events such as deletions in different tissues[28,29], including the human brain[30]. However, this method has also received a lot of criticism as a quantitative assay due to possible technical artifacts (e.g. variations in template DNA concentration) that can lead to the misinterpretation of LX-PCR results[31]. The only alternative source of information that may help resolving this puzzle has been offered through the analysis of AD brain tissues where much of the increased mtDNA was ultrastructurally segregated in autophagocytic compartments and therefore unavailable for PCR amplification[14].

We also tried to verify a positive correlation between the quantitative variation of the mitochondrial genomeand possible alterations in terms of mass and shape of the overall mitochondria. Measurements of integrated fluorescence area for the evaluation of total mitochondrial mass revealed a slight, though statistically significant, decrease of the overall content of mitochondria in case of Ab exposure. This finding is consistent with the absence of clear morphological alterations of mitochondria such as swelling or fragmentation. Indeed, without any *de novo* mitochondria biosynthesis, only enlargements of mitochondria could eventually account for a total increase in the TMRM (tetramethyl rhodamine methyl ester) stained fluorescent area. Despite the fact that the morphology and dynamics mitochondria have tissue and cell specific features[32], *in vivo* image analysis has shown a direct correlation between mitochondrial DNA depletion and disruption of the mitochondrial reticulum, which resulted in formation of vesicular organelles with circular cristae[33]. A confirmation of this phenomenon has emerged from description of individual mitochondria changing their morphology in accordance with mtDNA redistribution and intimate relationship to cell cycle phases[34].

Some previous reports have shown that, in comparison to controls, an approximately eightfold increase in morphologically abnormal (swelled or enlarged) mitochondria after six passages of cybrid cell lines from sporadic AD subjects[35]. In contrast to these reports, we have demonstrated that up-regulation of the mitochondrial genome does not necessarily imply either such a great increase of mitochondrial mass or an impairment of normal morphology. This result is relevant since it is supposed that low levels of Ab would have mtDNA as a

primary target before the appearance of the irreversible damage of mitochondrial filaments. At this point it should be clarified that in our model we circumvented possible unspecificity of TMRM due to inefficient uptake or the ongoing efflux mediated by MDR pumps upon Ab treatment by using EYFP cytochrome c oxidase transfected cells. This method has been extensively used to track mitochondria because of the transmembrane distribution of the enzyme. Cytochrome c oxidase-tagged mitochondria were also resistant to the toxic effects of Ab because the continuity of fluorescence pattern was unchanged even after the amyloid insult. This finding confirmed earlier notion that in physiological conditions the reticular form better drives rapid transmission of energy through the propagation of a membrane potential and therefore facilitates energy delivery from the cell periphery to the cell core[36].

Finally, since a recent review[37] proposed a »chameleon « role for Ab (a phenomenon obviously dependent upon Ab concentration which, in turn, determines *in vitro* fibrillization rate), always swinging between the prooxidant and anti-oxidant activities, in this study we also investigated if $Ab_{1–42}$ exposure is *per se* a biochemical inducer of DNA oxidation. Although some previous reports found 8OHdG-immunopositive neurons in AD brain sections[12], we have found no experimental evidence in neuronal cell culture to support this view. Since in our model we observed a steady-state level of 8OHdG immunoreactivity, our results are consistent with the antioxidant role of $Ab_{1–42}$ when applied at concentrations lower than 10 mM. These data were also validated by the minimal fraction of cells that were committed to cell death (data not shown), and are in accordance with the published observations where 5 mM Ab induced only 15% decrease in the viability properties of SY5Y cells, as compared to controls[38].

Recent advances in model studies of AD have revealed that Ab and other amyloid precursor protein (APP) derivatives (particularly mutated ones) are key factors which enter into mitochondria and induce the generation of free radicals and oxidative damage in AD neurons[5]. Evidence from biochemical and gene expression studies has also suggested that mitochondrial abnormalities *per se* are critical for the initiation of late-onset sporadic AD[4]. However, the precise causal links between mitochondrial abnormalities and synaptic damage-based cognitive decline are still unknown. Since currently approved drugs for AD (acetylcholinesterase inhibitors tacrine, galantamine, donepezil and rivastigmine and non-competitive antagonist of NMDA receptors memantine) provide only temporary relief of some symptoms of dementia and do not modify AD pathology, there is an urgent need for development of alternative therapeutic strategies. Antioxidants tested so far were found to be safe, had few adverse effects, readily crossed blood brain barrier and appear to be a promising mitochondrial medicine to improve cognitive functions of AD patients[5]. In this context, the results reported here may serve as a starting point for development of more sophisticated models of beta amyloid toxicity in which the action of anti-oxidative compounds could be tested. On the other side, it would be of particular relevance to test how modulation of metal ions (such as copper, zinc and iron) reduction affect mitochondrial DNA oxidation in the presence of minimal amounts of fibrillogenic Ab.

Acknowledgements

This work was supported by The Italian Ministry of Health (MINSAN/RC 1999 – IRCCS Neurologico C. Mondino, Pavia), the European Community (European Social Fund, contract number 37/5428 1999), the Regione Autonoma della Sardegna (LR 26/96, PVS 2001) and grant no. 0108-1081870-1942 from MZOŠ RH to GŠ. The authors wish to thank: Prof. Giacomo Diaz from the Department of Cytomorphology, University of Cagliari, for his skillful assistance for the image analysis experiments and the statistical guidance, Prof. Juan Llopis from University of Castilla-La Mancha, Albacete (Spain) for providing the cytochrome

c oxidase-EYFP plasmid, and Ian Holt from RJAH Orthopaedic Hospital, Oswestry (UK) for critical reading of the manuscript.

REFERENCES

1. HARDY JA, HIGGINS GA, Science, 256 (1992) 184. —
2. VICKERS JC, DICKSON TC, ADLARD PA, SAUNDERS HL, KING CE, MCCORMACK G, Prog Neurobiol, 60 (2000) 139.—
3. RAINA AK, HOCHMAN A, ICKES H, ZHU X, OGAWA O, CASH AD, SHIMOHAMA S, PERRY G, SMITH MA, Prog Neuropsychopharmacol Biol Psychiat 27 (2003) 251.—
4. REDDY PH, BEAL MF, Brain Res Rev, 49 (2005) 618.—
5. REDDY PH, J. Neurochem, 96 (2006) 1. —
6. MIRANDA S, OPAZO C, LARRONDO LF, MUNOZ FJ, RUIZ F, LEIGHTON F, INESTROSA NC, Prog Neurobiol, 62 (2000) 633. —
7. BEHL C, DAVIS JB, LESLEY R, SCHUBERT D, Cell, 77 (1994) 817. —
8. HENSLEY K, CARNEY JM, MATTSON MP, AKSENOVA M, HARRIS M, WU JF, FLOYD RA, BUTTERFIELD DA, Proc Natl Acad Sci, 91 (1994) 3270. —
9. MECOCCI P, BEAL MF, CECCHETTI R, POLIDORI MC, CHERUBINI A, CHIONNE F, AVELLINI R, ROMANO G, SENIN U, Mol Chem Neuropathol, 31 (1997) 53.
10. LEZZA AM, MECOCCI P, CORMIO A, BEAL MF, CHERUBINI A, CANTATORE P, SENIN U, GADALETA MN, FASEB J, 13
(1999) 1083. —
11. NUNOMURA A, PERRY G, PAPPOLLA MA, FRIEDLAND RP, HIRAI K, CHIBA S, SMITH MA, J Neuropathol Exp Neurol, 59 (2000) 1011. —
12. NUNOMURA A, PERRY G, ALIEV G, HIRAI H, TAKEDA A, BALRAJ EK, JONES PK, GHANBARI H, WATAYA T, SHIMOHAMA S, CHIBA S, ATWOOD CS, PETERSEN RB, SMITH MA, J Neuropathol Exp Neurol, 60 (2001) 759. —
13. SUTER M, RICHTER C,
Biochemistry, 38 (1999) 459.
14. HIRAI K, ALIEV G, NUNOMURA A, FUJIOKA H, RUSSELL RL, ATWOOD CS, JOHNSON AB, KRESS Y, VINTERS HV, TABATON M, SHIMOHAMA S, CASH A, SIEDLAK SL HARRIS PLR, JONES PK, PETERSEN RB, PERRY G, SMITH MA, J Neurosi, 21 (2001) 3017. —
15. DE LA MONTE SM, LUONG T, NEELY TR, ROBINSON D, WANDS JR, Lab Invest, 80 (2000) 1323. —
16. WEI
YH, LEE CF, LEE HC, MA YS, WANG CW, LU CY, PANG CY, Ann NY Acad Sci, 928 (2001) 97. —
17. LEE HC, YIN PH, LU CY, CHI CW, WEI YH, Biochem J, 348 (2000) 425. —
18. Lee HC, Yin PH, Lu CY, Chi CW, Wei YH, J Biomed Sci, 9 (2002) 517. —
19. NAKAMURA J, PURVIS ER, SWENBERG JA, Nucleic Acid Res, 31 (2003) 1790. —
20. LUETJENS CM, LANKIEWICZ S, BUI NT, KROHN AJ, POPPE M, PREHN HM, Neuroscience, 102 (2001) 139. —
21. HURT EC, PESOLD-HURT B, SUDA K, OPPLIGER W, SCHATZ G, EMBO J. 8 (1985) 2061. —
22. MATSUYAMA S, LLOPIS J, DEVERAUX QL, TSIEN RY, REED JC, Nature Cell Biol, 2 (2000) 318.—
23. BLIN N, STAFFORD DW, Nucleic Acid Res, 3 (1976) 2303. —
24. CHENG S, HIGUCHI R, STONEKING M, Nature Gen, 7 (1994) 350. —
25. SWERDLOW RH, KISH SJ, Int Rev Neurobiol, 53 (2002) 341. —

26. CARDOSO SM, SANTANA I, SWERDLOW RH, OLIVEIRA CR, J Neurochem, 89 (2004) 1417. —
27. MANCZAK M, ANEKONDA TS, HENSON E, PARK BS, QUINN J, REDDY PH, Hum Mol Genet, 15 (2006) 1437. —
28. MELOV S, SHOFFNER JM, KAUFMAN A, WALLACE DC, Nucleic Acids Res, 20 (1995) 4122. —
29. MELOV S, HINERFELD D, ESPOSITO L, WALLACE DC, Nucleic Acid Res, 25 (1997) 974. —
30. MELOV S, SCHNEIDER JA, COSKUN PE, BENNETT DA, WALLACE DA, Neurobiol Aging, 20 (1999) 565. —
31. KAJANDER OA, KUNNAS TA, PEROLA M, LEHTINEN SK, KARHUNEN PJ, JACOBS HT, Biochem Biophys Res Commun, 254 (1999) 507. —
32. BEREITER-HAHN J, Int Rev Cytol, 122 (1990) 1. —
33. GILKERSON RW, MARGINEANTU DH, CAPALDI RA, SELKER JML, FEBS Lett, 474 (2000) 1. —
34. MARGINEANTU DH, COX WG, SUNDELL L, SHERWOOD SW, BEECHEM JM, CAPALDI RA, Mitochondrion, 1 (2002) 425. —
35. TRIMMER PA, KEENEY PM, BORLAND MK, SIMON FA, ALMEIDA J, SWERLOW RH, PARKS JP, PARKER WD, BENNETT JP, Neurobiol Dis, 15 (2004) 29. —
36. SKULACHEV VP, TIBS 26 (2001) 23. —
37. ATWOOD CS, OBRENOVICH ME, LIU T, CHAN H, PERRY G, SMITH MA, MARTINS RN, Brain Res Rev, 43 (2003) 1. —
38. PAPPOLLA MA, CHYAN YJ, POEGGELER B, BOZNER P, GHISO J, LEDOUX SP, WILSON GL, J Pineal Res, 27 (1999) 226.

A. Diana
Department of Cytomorphology, University of Cagliari, Cittŕ Universitaria di Monserrato, 09042 Monserrato, Italy
e-mail: diana@unica.it

Legends

Fig. 1. Distribution of anti-8OHdG immunofluorescence. a: Under basal conditions, 8OHdG-like immunolabeling is strongly detected in the cytoplasmic domain while nuclei reveal very low immunoreactivity. Notably, the largest cells contain a granular fluorescent signal spread over the abundant cytoplasm. Some neurites are also stained by the anti-8OHdG antibody. b: Cells exposed to Ab1–42 are also immunopositive regardless to the cell size. Scale bar = 10 μM

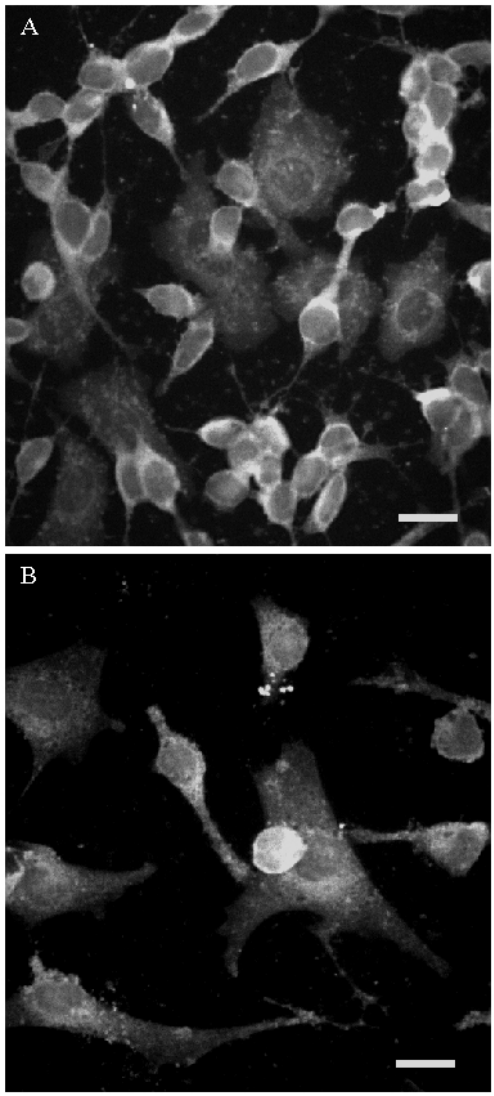

Fig. 2. Mitochondria distribution and shape upon Mitotracker uptake. a: Control cells display a reticular organization of mitochondria filling the whole cytoplasm, but rarely reaching the neuritic processes. The highest peaks of fluorescence are obtained possibly due to overlapping of mitochondrial elements. b: In Ab1-42 treated cells, the overall architecture of mitochondria was unaltered as compared to control cells, albeit with the additional feature of isolated cells being more sensitive to photobleaching. c: Incubation of neuroblastoma cells in hypotonic solution affects the continuity and size of fluorescent mitochondria. As a result, fragmented and swollen structures can be observed. Scale bar = 10 μM.

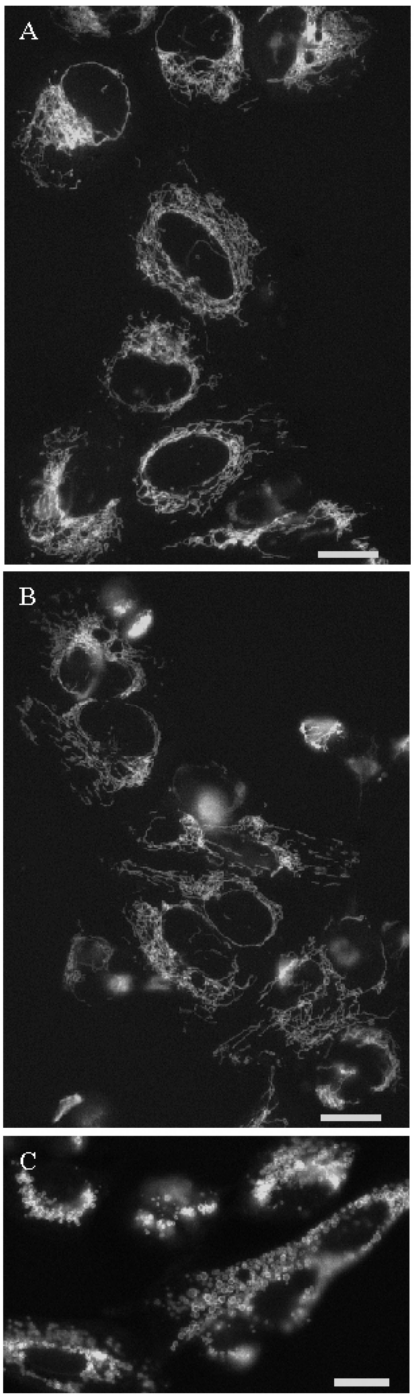

Fig. 3. EYFP-tagged cytochrome c oxidase protein expression in living cells. a: The distribution pattern in control cells is consistent with the specific accumulation within the mitochondria. Mitochondria are represented by a mesh of filaments sometimes detectable in the shape of single string. b: Ab1–42 has no effect on EYFP labeled mitochondria. The fluorescent dots could be occassionally detected, probably due to the initial storage of the cytochrome c oxidase. Scale bar = 10 μM.

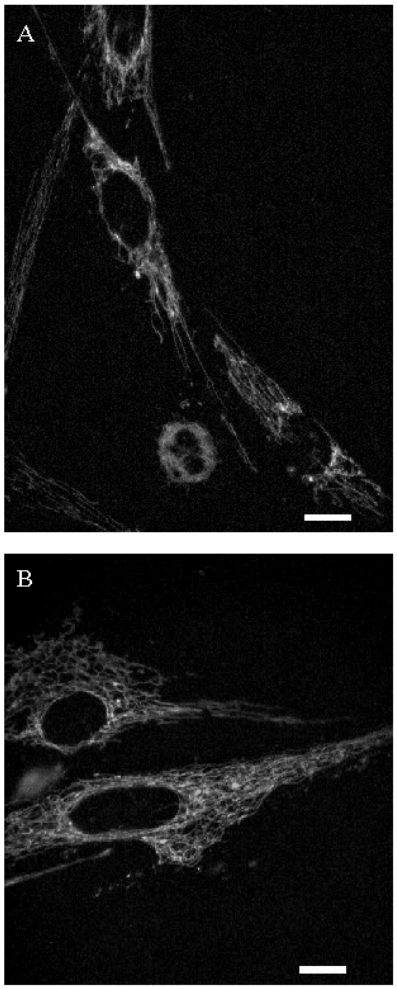

Fig. 4. SYBR Green stained gel of LX-PCR using DNAs from two different experiments (see text for explanation). Specific bands representative of the entire mitochondrial genome (16.3 Kb) exhibited the strongest signal in the Ab1–42 samples. A smear of fragments above or below 16.3 Kb was more enhanced in the presence of Ab1–42. The additional band between 10 and 8.6 Kb was more evident in DNAs of treated cells. Duplicate experiments of control and Ab1–42 DNAs were indicated as C1, C2 and Ab1, Ab2 respectively.

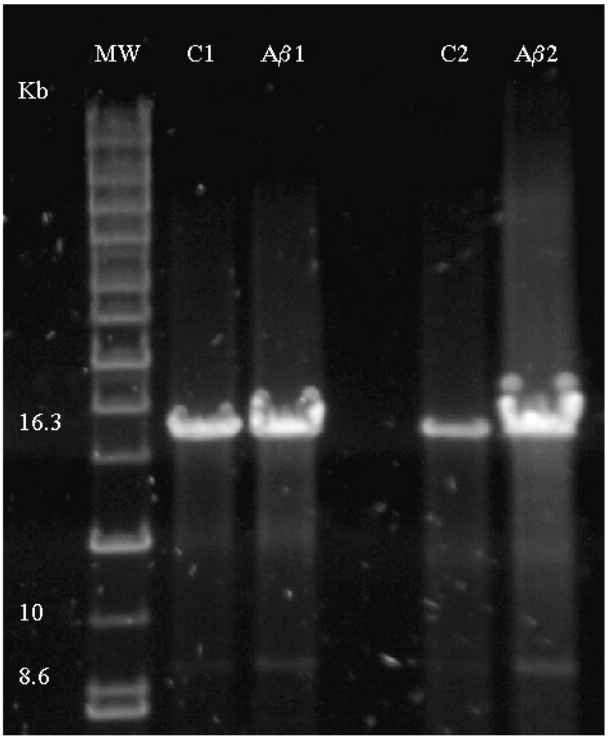

MORFOLOGIJA I STANJE DNA MITOHONDRIJA NAKON SUBLETALNE EKSPOZICIJE PEPTIDOM BETA-AMILOIDA$_{1–42}$

SAŽETAK

U mozgova osoba s Alzheimerovom bolešću (AD) vidi se veliki spektar mitohondrijalnih promjena kako na morfološkoj, tako i na genetskoj razini. U staničnim modelima AD pronađena je kauzalna povezanost između prisutnosti peptida beta-amiloida (Ab) i disfunkcije mitohondrija samo uz upotrebu koncentracija Ab koje su sposobne izazvati masivnu smrt neurona. No, mitohondrijalne promjene povezane sa subletalnom ekspozicijom Ab nisu tako dobro proučene. U ovom smo istraživanju pokazali da subtoksična ekspozicija s 1 mM Ab$_{1–42}$ ne mijenja oblik mitohondrija stanica u kulturi, što je jasno vidljivo nakon vizualizacije mitohondrija pomoću na razlike u potencijalu neosjetljive fluorescentne probe Mitotracker Green i na temelju ekspresije citokrom c oksidaze označene modificiranim žutim fluorescentnim proteinom s poboljšanom emisijom (EYFP). Imunolokalizacija oksidativnih kompleksa 8-hidroksi-2'-deoksigvanozina, 8-hidroksigvanina i 8-hidroksigvanozina pokazala je da jednomolarna koncentracija Ab$_{1–42}$ također nije dovoljna da bi izazvala dramatične kvalitativne promjene vizualiziranih oksidativnih produkata RNA i/ili DNA. Ipak, u usporedbi s kontrolama, semikvantitativnom analizom mitohondrijalne mase izmjerene iz intenziteta ukupne fluorescencije otkrili smo značajne razlike koje ukazuju da dolazi ili do sveukupnog smanjivanja biosinteze mitohondrija ili pak da se radi o pojačanoj autofagičkoj eliminaciji stanica tretiranih s Ab. Nadalje, upotrebom lančane reakcije polimeraze dugog odsječka (long range PCR) u stanica tretiranih s Ab pronašli smo značajan porast cijele mitohondrijalne DNA (mtDNA). Ovakva pojačana sinteze cijele mtDNA bila je popraćena izraženom fragmentacijom neamplificirane mtDNA, vjerojatno uslijed štetnog djelovanja Ab. Dobivene rezultate interpretirali smo kao niz kompenzatornih procesa izazvanih oštećenjem mtDNA, kojima je cilj zaustavljanje naglog porasta oksidacije. Zaključno, naši nalazi ukazuju da bi rane terapijske intervencije usmjerene na prevenciju oksidativnog oštećenja mitohondrija mogle odgoditi progresiju AD i pomoći u liječenju bolesnika s AD.